

RESEARCH

Open Access



# Multi combination pattern labeling by using deep learning for chameleon rotary machine environment

JiEun Kang<sup>1†</sup>, SuBi Kim<sup>1†</sup> and YongIk Yoon<sup>1\*</sup>

<sup>†</sup>JiEun Kang and SuBi Kim are equally contributed to this work.

\*Correspondence: yiyoon@sookmyung.ac.kr

<sup>1</sup> Department of IT Engineering, Sookmyung Women's University, 100, Chungpa-ro 47 gill, Yongsan-qu, 04310 Seoul, Korea

## Abstract

Rotary machines are constructed and operated in diverse industrial environments and operate according to various specifications and characteristics. When rotary machinery constructed under dynamic real world environments is in operation, various types of vibrations are generated depending on the normal or defective state of the machinery. In this way, Numerous studies have been conducted on vibration analysis for diagnosing the state of rotary machinery. However, Without performing robust data cleansing and comprehensive labeling of the internal and external state of complex machinery, the analysis process of the condition monitoring system faces difficulties in accurately identifying the various and complex states of rotary machines and making decisions in the dynamic real world. To overcome these limitations, this paper proposes Multi Combination Pattern Labeling (MCPL) method. By simultaneously considering the complex internal and external states of rotary machines, MCPL generates detailed vibration frequency pattern criteria and labels for each state. Based on these complex pattern classifications, it is able to classify various types of abnormal states. The MCPL generates FFT patterns and spectrogram patterns by considering the simultaneous internal and external states of the rotary machine. Extracting internal and external patterns, each pattern is combined for identifying convergence patterns, named MCP. Each MCP proceeds labeling process, named MCPL, then MCPL dataset is structured. MCPL dataset is verified based on Deep Neural Network (DNN) and Convolutional Neural Network (CNN). By utilizing the DNN and CNN techniques to derive MCPL from MCP, it becomes possible to perform unbiased state diagnosis across a variety of patterns, based on the complex patterns of the internal and external states of the rotating machinery. Presenting high accuracy and stable results, MCPL are able to classify rotary machine states and detect anomalies under the convergence environment. Our source code and utilized data are available on <https://github.com/JEESBSB/Journal-of-Big-Data>.

**Keywords:** Fast fourier transform, Short-time fourier ransform, Spectrogram, Deep learning, Deep neural network, Convolutional neural network, Multi-combination pattern labeling, Machine troubleshooting

## Introduction

Rotating machines operating power account for more than 50% of the world's electricity consumption in the industrial environment [1]. These machines consist of different driving capacities and they are operated by various parts of machines such as bearings, shafts, rotating bodies, belts, etc [2]. Rotary machines are categorized into small, medium, and large sizes based on their driving capacity. Specifically, machines with a power output below 15 kW are considered small, those with a power output ranging from 15 kW to 300 kW are classified as medium, and machines with a power output between 300 kW and 50 mW are categorized as large. While rotating machines are in operation, vibration is produced by rotational power and various inherent vibration characteristics and patterns appear depending on the condition of the rotating machine. While rotating machines are in operation, vibration is produced by rotational power and various inherent vibration characteristics and patterns appear depending on the condition of the rotating machine. However, the vibration patterns of a rotary machine exhibit various types not only for each fault in its components but also for each driving capacity. As the International Organization for Standardization (ISO) suggests acceptable RMS and PEAK values for maintenance activities based on standard vibration information considering the size of the machine, the range of vibration and allowable range can vary depending on the operating power of the device.

Research on fault detection and condition diagnosis of rotating machinery assumes that vibration data is collected for a single machine, despite the fact that rotating machinery is operated in various fields. [3–5] Also, even though the data is collected from different machines, there are diagnosed as the same failure without considering external factors, leading to limitations in diagnosing various parts for failures in diverse environments. The fault detection in rotary machines without simultaneously considering the internal and external environments of machines used in various domains has limitations in identifying detailed vibration types, which may result in misidentification and Misdiagnosis of fault types as a different state even though it is the same state depending on the driving capacity.

Furthermore, performing a diagnostic on the condition of rotary machine without considering various internal and external vibration patterns may lead to unpredictable machine shutdowns and accidents, resulting in unexpected industrial and economic losses as well as fatal accidents and human casualties. For example, faults in rotary machines such as bearing defects or loose belts may not initially cause visible issues, but leaving them unchecked can lead to more significant problems over time. In the case of bearing defects, frictional forces arise at the contact points, while loose belts have insufficient tension and cause vibration. Both of these can initially cause slight noise and vibration, as well as heat generation, but if left unattended, they can lead to bearing and belt failure, resulting in complete failure of the rotating machinery. Failure to accurately identify the faults in the rotary machine and take appropriate measures in advance can ultimately result in a complete failure of the rotating machinery.

Therefore, a detailed diagnostic approach that takes into account the internal state and operational environment of rotating machines is necessary to accurately identify complex vibration patterns and their corresponding labels. This enables unbiased, immediate, and precise condition diagnosis and decision-making even for various data patterns.

The Multi Combination Pattern Labeling(MCPL) methodology proposed in this paper considers both the internal rotary machine’s components and external driving capacity of rotary machine to generate and combine detailed vibration patterns and labels for each state, aiming to diagnose the state of the rotary machine with high reliability. The MCPL enables the construction of learning datasets based on flexible patterns and labeling, and the extraction of patterns and classification of labels through highly accurate learning dataset makes it possible to obtain unbiased and reliable results.

The following sections are described and represented as follows. Firstly, “Multi-Combination Pattern Labeling(MCPL) Model” section shows MCPL architecture and illustrated method of each step. Thereafter, “MCPL Algorithm” section demonstrates MCPL implemented process algorithms based on proposed pattern extraction method. “Verification of MCPL model” section experiments classification of rotary machie states and anomaly detecrion and verifies MCPL dataset based on MCPL labels resulted from MCPL algorithm. Finally, “Conclusion and future work” section concludes with summary of this study and shows future direction for this work.

**Related work**

Recent technological breakthroughs of IT, such as Internet of Things, sensors, networks, and computer vision, have allowed monitoring the current mechanical state by collecting and processing vibration signal data from sensors attached to lots of kind of objects [6–10]. Using the collected vibration signal data, vibration patterns from vibration signal frequency can diagnose current machine states and detect abnormal parts of machines real-time. To determine and classify the abnormal conditions, there are various vibration pattern extraction methods. Common methods for extracting vibration patterns include: (1) time domain feature extraction techniques using statistical values such as mean, variance, skewness, and kurtosis in time domain, and physical values such as RMS (Root Mean Square) and Peak-to-Peak [5, 11, 12]. (2) frequency domain feature extraction techniques such as fourier transform (TF) [5, 11, 13] transforming time domain into frequency values, short-time fourier transform (STFT) [14–16] extracting time-frequency values by calculating frequency components for each time interval, and wavelet transform [17–19] simultaneously adjusting both frequency and time resolution. In addition, classification methods include binary classification model [3] that determines normal and failure states according to vibration feature values, a multi-classification model [20, 21] that can classify the various kind of faults, and deep learning-based classification

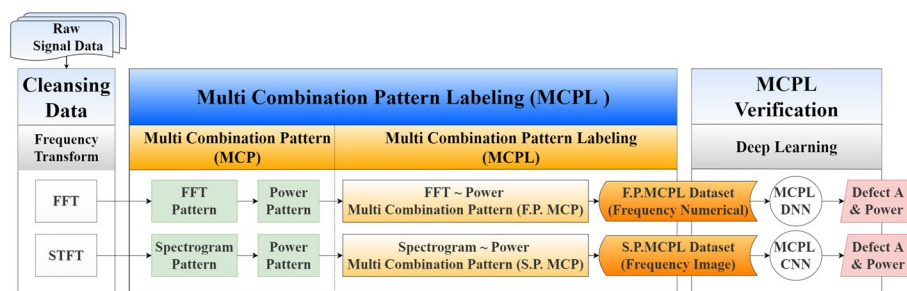


**Fig. 1** MCPL model architecture

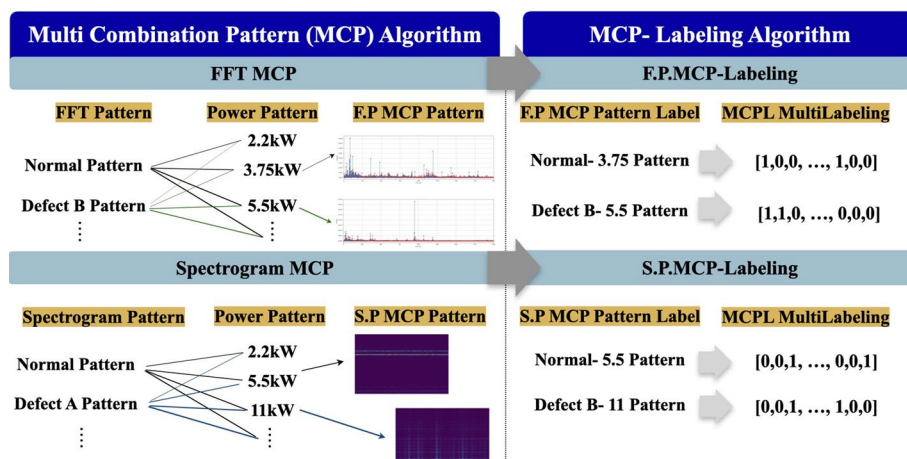


Fig. 2 MCPL technique

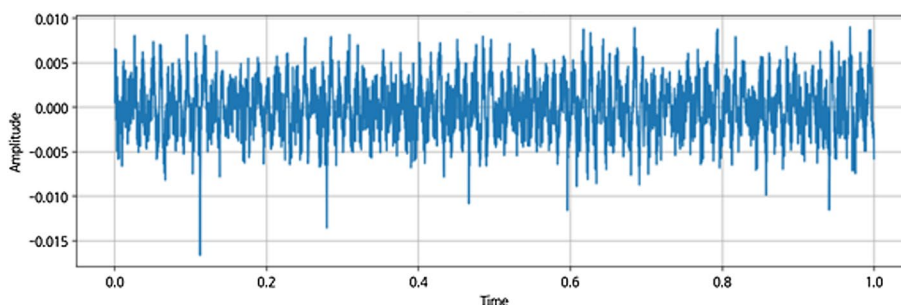


Fig. 3 Original vibration signal data graph

model using spectral images [16, 22, 23] according to the development of computer vision technology.

Kafeel et al. [3] proposed a system for detecting healthy and faulty states of rotary machines using vibration signal analysis based on vibration data collected from 45KW three-phase induction motors. K.Gu et al. [20] proposed a smart fault-detection approach that converts vibration data in the time domain to the chaotic domain to generate 3D correlation features and extracts features through the Euclidean feature value(EFV) method for classifying four typical states of industrial bearings(normal state, outer ring faults, inner ring faults, and ball faults). M.J. Hasan et al. [22] generated composite color image through a signal-to-image conversion technique by fusing information from multi-domains and extract the characteristics of bearing failures trained a CNN to classify four states.(normal type (NT), inner raceway type (IRT), outer raceway type (ORT), and roller type (RT)).

Furthermore, fault classification technique are currently being researched for enhance the accuracy using various techniques, including signal data conversion, expansion of unbalanced datasets [24], utilization of small sample data [25], identification of new defect conditions and new pattern relearning [26].

J. Li et al. [24] proposed a DARNN-CBAM-CNN model that diagnoses rolling bearing defects to solve the imbalanced datasets of existing studies have a limitation that

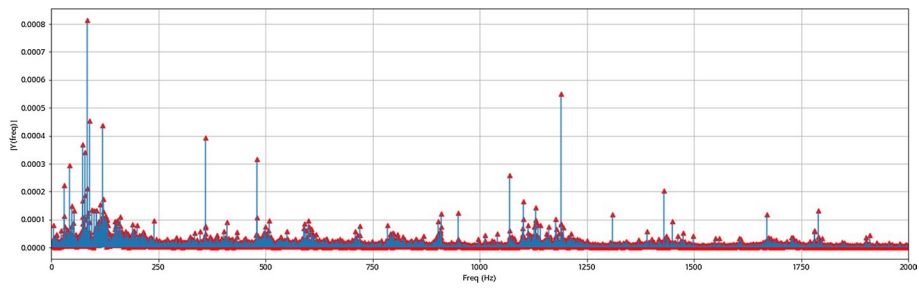


Fig. 4 FFT data graph

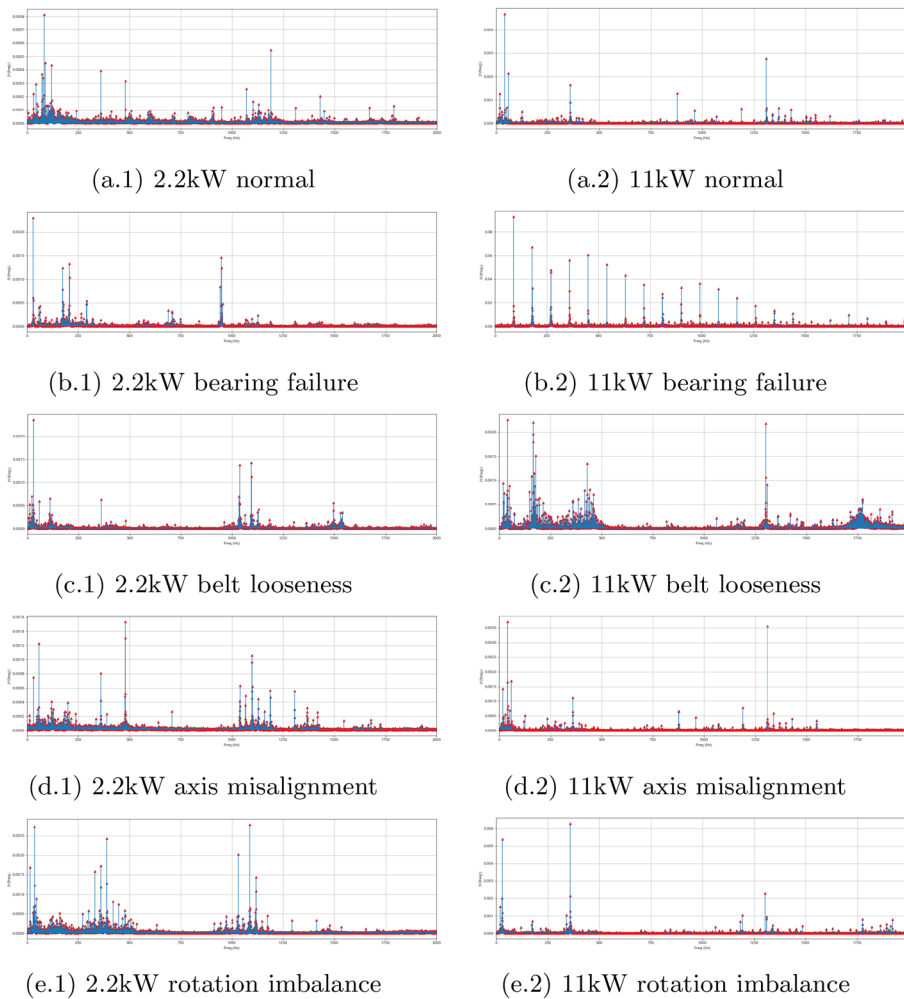


Fig. 5 FFT graphs showing the differences in vibration patterns by capacity based on FFT

number of normal and fault sample is assumed to be same or similar. The DA-RNN(Dual-stage Attention-based Recurrent Neural Network) expands imbalanced datasets, and CNN(Convolution Neural Network) model with an embedded CBAM(Convolutional Block Attention Module) structure classify fault using images converted from vibration signals. Under imbalanced data conditions, the proposed method achieves improved diagnosis accuracy compared to other intelligent fault diagnosis methods, such as those based on a neural networks, a machine learning, deep learning, and a DARNN-CNN without using CBAM.

Anil Kumar et al. [25] presented a Novel Convolutional Neural Network(NCNN) for identifying bearing faults in rotary machinery from small datasets. The NCNN modifies the cost function of convolution neural network(CNN) to add sparsity cost to avoid unnecessary neuron activations in the hidden layer and combines modified CNN with transfer learning to identify bearing faults in small training samples. The proposed combination function shows better performance, with an accuracy of 91%, compared to a performance without transfer function learning which has an accuracy of 51%.

Wu et al. [26] identified novel defect conditions that previously undiscovered faults and learned new patterns through the convolutional neural networks and autoencoder (CNN-AE) based incremental learning method. The signal data for normal and known Severity Level 1, unknown Severity Level 2 of two defects(misalignment, unbalanced) collected based on machinery fault simulator (MFS) are converted to spectrogram to label the fault situation with the working condition information of the rotating machine, and classify known defects and detect new patterns using the proposed model. As a result of the experiment, the proposed model shows high performance in accurately detecting and identifying previously novel defects even if a novel defect condition is discovered through gradually trained.

As observed, majority studies on fault classification and prediction in rotary machines suggest methods to more accurately identify bearing faults, which represent the most common type of faults in these machines. [21, 25, 27] Rotary machines are operated by various combinations of components and driven in different environments, yet existing studies classify only one or some components in a predetermined machine environment, resulting in limited flexibility for unexpected vibration types and patterns. Therefore, this paper proposes the MCPL labeling technique that considers both internal and external factors simultaneously.

### **Multi-combination pattern labeling(MCPL) model**

This paper suggests MCPL to solve the limitation of vibration pattern not considering various parts of machine and operation capacity state in the same time. The advantage of MCPL is possible to consider multi-environmental aspects of rotary machines. MCPL produces robust multi combination patterns and labels capable of identifying both the inner vibration patterns of rotary machine parts and the external vibration patterns at the same time, resulting in fluent and trustworthy dataset reflecting dynamic

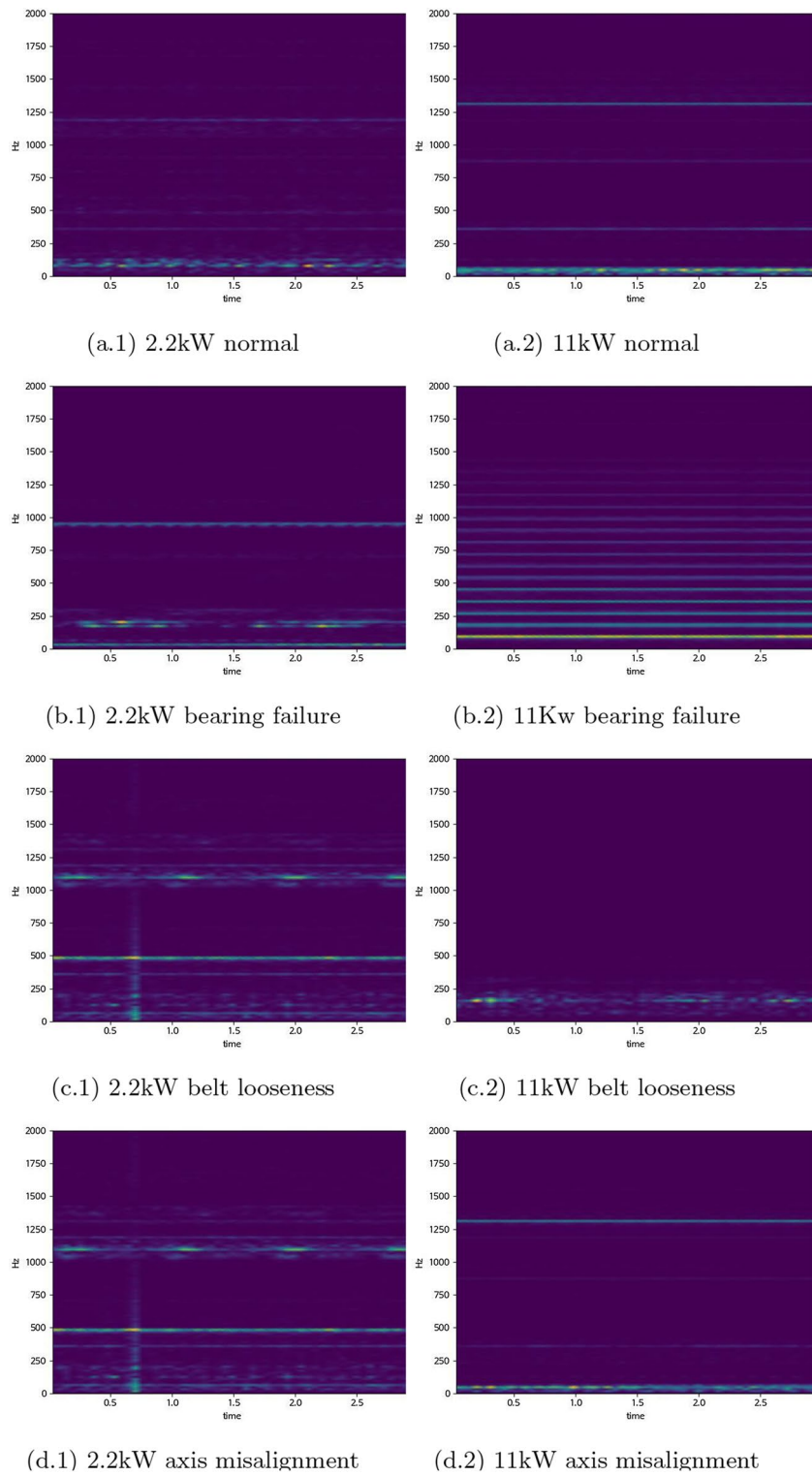


**Fig. 6** Graphs showing the differences in the vibration pattern by capacity based on spectrogram

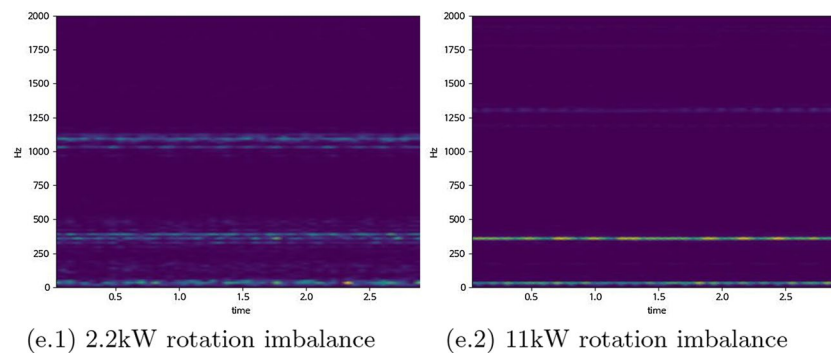


**Fig. 6** continued

environments. Therefore, MCPL dataset is capable of classifying detailed vibration types and conducting situation-adaptive state diagnostics, without the limitation of specific type of rotary machines and operational environment. This section describes the whole process of the MCPL model for generating MCPL labels and datasets, from the process of collecting data to the process of verifying the MCPL label dataset verification. Figure. 1 shows the entire process of the MCPL architecture. The process comprises four primary steps: Step 1 involves collecting raw signal data, followed by step 2, which involves data cleansing. Step 3 entails the use of Multi Combination Pattern Labeling (MCPL), and finally, in step 4, MCPL anomaly detection is performed. Figure. 1 shows the whole process of MCPL architecture.

- **Raw signal data:** The vibration raw signal data are collected from rotating machines. In the vibration signal data, only vibration waveform information is represented under the time domain. In the case of vibration generated from the rotating machine, it is available to identify current states of machine through vibration specific frequency domain and its values. So, MCPL model perform cleansing data process, which is the process of frequency transformation.
- **Cleansing data:** MCPL first performs Fast Fourier Transform (FFT) and Short Time Fourier Transform(STFT) based frequency transformations process. The converted frequency values are input to MCPL to identify frequency patterns.
- **Multi Combination Pattern Labeling(MCPL):** MCPL has two modules, one is Multi Combination Pattern(MCP) module and the other is Multi Combination Pattern Labeling(MCPL) module. In the MCP module, FFT patterns are extracted from FFT values and Spectrogram patterns from STFT frequency images. After the FFT patterns and Spectrogram patterns process, the Power pattern reflecting the outside environment of the rotary machine is identified from the FFT patterns and Spectrogram patterns. Each FFT pattern and Spectrogram pattern is combined with a Power pattern named the FFT-Power Multi Combination Pattern(F.P.MCP) and Spectrogram-Power Multi Combination Pattern(S.P.MCP). F.P.MCP and S.P.MCP input to the MCPL module. The MCPL module is a labeling process generating labels for the standard of the operating rotary machine's state from combination patterns including inner and outside frequency information. Then F.P. MCPL and S.P.MCPL datasets are constructed. F.P.MCPL and S.P.MCPL are available for outlier detection and

classification of rotary machine state according to inner vibration pattern types with outer vibration frequency patterns.

- **MCPL anomaly detection:** MCPL anomaly detection verifies F.P.MCPL and S.P.MCPL datasets through a deep learning anomaly detection process. DNN is applied for F.P.MCPL datasets and CNN for S.P.MCPL datasets. Deep Learning classifies labels to identify the rotary machine states and then the accuracy represents how well construct datasets from the MCPL process.

### **Data cleansing**

Data cleansing converts the vibration signal data values to the frequency domain for estimating the magnitude values of the frequency domain. In the data cleansing process of FFT, the frequency domain and the size of each frequency domain were stored. In STFT, Spectrogram images are extracted based on STFT values which visualize frequency differences by the color density. Each of them becomes input data for the MCPL algorithm.

### **Multi combination pattern**

The vibration data of the rotating machine is collected in chronological order, it was difficult to extract the characteristics to conduct an intrinsic semantic analysis only the vibration frequency values. In the case of vibration, the frequency pattern depends on the cause of frequency appearance situations. Thus, it is possible to identify vibration appearance types reflecting the machine's states based on the frequency patterns. MCP module performs a pattern extraction process for frequency rotating machines' inner and outside situation cognition. FFT patterns are derived from FFT values and Spectrogram Patterns are induced from Spectrogram images. Both reflect the vibration frequency patterns of the inner situation when rotating machines are in operation. Power patterns result from rotating machines' power capacity, and outside information, representing rotating machines structured standards. After Pattern extraction, FFT ~ Power MCP and Spectrogram ~ Power Patterns MCP are generated by each of FFT Patterns and Spectrogram Patterns combining with Power patterns.

### ***Fourier transform-based FFT pattern***

The FFT pattern method involves the extraction of a frequency pattern based on the frequency values and the magnitude value of each frequency value. It is possible to classify the state of the rotating machine and detect outlier situations or patterns from specific vibration magnitude change and harmonic generation at specific frequency values.

### ***STFT-based spectrogram pattern***

In the spectrogram pattern method, First SFTF is conducted for frequency transform. It considers the time domain and frequency domain at the same time. So the time domain of raw data is divided into several sections and then frequency conversion is performed to deduce the frequency magnitude per time in the frequency domain.

After STFT, spectrogram images are generated, and it is available to visualize the frequency values. From the spectrogram, frequency patterns are extracted which is possible to consider the frequency values based on the time domain. The spectrogram is expressed in different colors depending on the magnitude of the frequency value, and color patterns in the spectrogram allow the classification of the state of the rotating machine and the decision of outlier criteria.

#### **Power pattern**

The capacity of a rotating machine depends on its size. The magnitude of the frequency value varies concerning the capacity of the rotating machine, which exhibits different frequency pattern characteristics according to the power capacity representing the external machine information environment. Owing to these characteristics, even though the vibration data are collected from a rotating machine in the same state, the vibration frequency pattern is different with the same rotating machine state. In this study, the frequency pattern for each capacity is identified in the power pattern process. Thus, MCP this paper suggests combines the vibration frequency pattern and capacity power pattern with the FFT pattern and spectrogram pattern, respectively. Through the MCP method, it is not only possible to diagnose the state of the rotating machine using the internal vibration frequency pattern of the rotating machine but also to simultaneously extract the frequency pattern according to capacity information, which is external information, so that even if a similar pattern is detected, it is possible to detect flexible frequency patterns with detailed evidence.

#### **Multi combination pattern labeling**

The detailed MCPL module shown in Fig. 2. MCPL divides into F.P. MCPL process based on FFT ~ Power MCP and S.P.MCPL based on Spectrogram ~ Power MCP. Each of MCPL modules performs generating labels possible to classify internal pattern and external pattern at the same time. After labeling process, the final dataset is constructed for recognition of rotating machines states and outlier detection decision criteria. The MCPL detects the frequency pattern from the combination pattern reflecting the vibration data collected inside from the machine during operating the machine and external rotary machine structured environment information. MCPL based labels presents more detailed and flexible situation recognition of rotary machines and outlier detection under dynamic environment frequency convergence patterns.

#### **Algorithm for MCPL(MCPL Algorithm)**

The data used in this study consisted of vibration data from mechanical facilities provided by AIHub, which were collected by vibration sensors attached to mechanical facilities installed in three urban railway stations(Daejeon Station, City Hall Station, Gapcheon Station). There are five types of rotating machine conditions including normal, bearing failure, rotation imbalance, axis misalignment, and loose belt which is operating states for each parts of rotary machine. Each vibration dataset consisted of

time and acceleration values and the length time of each data is 3 s which a sampling time is 4,000.

### FFT, Spectrogram pattern and power pattern

The FFT and spectrogram methods were used to verify the pattern difference based on capacity explained in “Multi Combination Pattern” Section. 12,000 values from each vibration sensor data were stored at intervals of 0.00025 s for 3 s. As the raw signal data is shown in Fig. 3, it is constructed time and signal magnitude. The time-based raw signal data is difficult to identify the vibration frequency characteristic, so FFT transform process is essential to identify the vibration attributes. Figure 4 shows the result of the FFT transform. As shown in Fig. 4, it is available to extract patterns while extracting frequency values at each frequency domain. The Figs. 5 and 6 show pattern differences between the capacity of machines from frequency patterns based on rotary machine states. It indicates the necessity of detailed frequency patterns by not only extracting frequency patterns based on rotary machine operating states, but frequency patterns according to the power capacity of the rotary machine.

### F.P.MCPL Algorithm

---

#### Algorithm 1: FFT Pattern MCPL Algorithm

---

```

Data: Raw Signal Vibration Data, Operation State, Environment State
Result: F.P.MC Pattern & F.P.MCPL Label
Def Data_Cleaning(Raw Sensor Signal Data):
  # Fast Fourier Transform(FFT) for analyzing the frequency component of a signal in the
  # time domain.
  FFT_state =  $\sin S_\theta + i \cos S_\theta$ 
  [frequency, frequency value] = FFT_state(Raw Sensor Signal Data) return frequency,
  frequency value
Def MCP_Labeling(Operation state, Environment state):
  O_state = Operation state
  E_state = Environment state
  # Subset of patterns
  {FFT Pattern}  $\supset$  {Power pattern 1 Power pattern 2 ... Power pattern n}
  # labeling multi combination pattern by operation and environment state
  for i in range (len(O_state)) do
     $O_i = O[i]$ 
    for j in range (len(E_state)) do
       $E_j = E[j]$ 
      MCP_Label =  $O_i \otimes E_j$ 
  return MCP_Label
Def F.P.MCPLDataset(frequency, frequency value, MCP Label):
  # Make F.P.MCPL dataset
  for n in range (len(MCPLabel)) do
    FFT_Pattern = frequency value[n]
    Label = MCP Label[n]
    F.P.MCPL_dataset[n] = [FFTPattern, Label]
  return F.P.MCPL_dataset
Def Build_DNN_Model(# Raw Sensor Signal Data, Operation State, Environment State):
  FPMCPPL_Model = DNN_network(
    F.P.MCPLDataset( Data_Cleaning(Raw Sensor Signal Data),
    MCP_Labeling(Operation State, Environment State)))
  return FPMCPPL_Model(Raw Sensor Signal Data)
Def FPMCPPL_Detection(FPMCPPL_Model, Raw Sensor Signal Data):
  # Pattern and Label Extraction using FPMCPPL_Model
  NewDataset = Data_Cleaning(Raw Sensor Signal Data)
  FPMCPPL_Model.predict(NewDataset) return F.P.MC Pattern, F.P.MCPL Label

```

---

This section describes the “FFT Pattern MCP algorithm” for the labeling process. There are five modules, the first module is Data Cleaning, which analyzes the signal in the time domain from raw sensor signal data generated within the rotary machine. This is achieved by decomposing the signal into sine and cosine wave functions through FFT, which transforms it into the frequency domain, and deriving the Fourier coefficients. The second module is the proposed Multi Combination Pattern Labeling(MCPL) technique, which derives combined labels by considering two states simultaneously, using the operation state and the environment state that represent the capacity of the previously labeled rotating machinery, as shown in Eq. (1). The third module generates a dataset for training by combining the Fourier coefficients(Input) extracted from the raw sensor signal data returned in the first module with the MCPL(Output) returned in the second module. The fourth module demonstrates the validation of the proposed F.P.MCPL by generating the FFT-based MCPL dataset through the trained DNN network using either a pre-generated dataset or real-time inputs of raw sensor signal data, operation state, and environment state. The details of building the model and verifying the MCPL will be described in the next chapter titled “Verification of MCPL model”. Verification of MCPL model. Finally, the system can be applied to classify the real-time state of rotary machine by converting incoming signal data into FFT patterns and loading the built model.

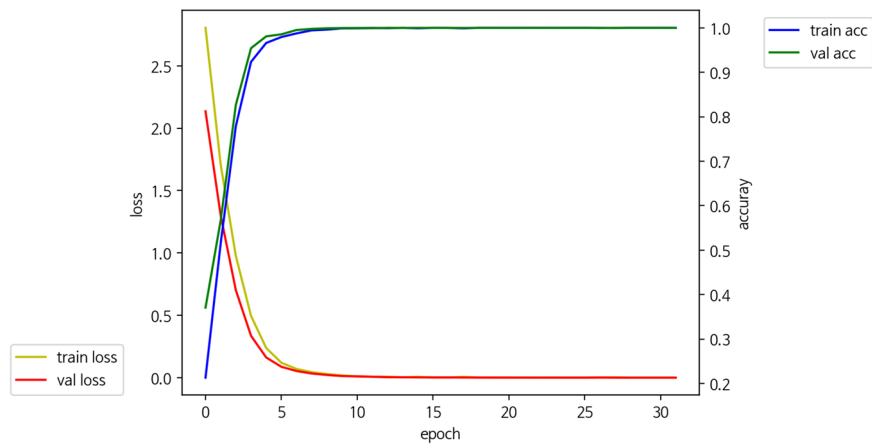
$$\begin{aligned}
 & \text{Operation State } O \otimes \text{Environment State } E \\
 & = \begin{pmatrix} o_{11} & o_{12} & \cdots & o_{1j} \\ o_{21} & o_{22} & \cdots & o_{2j} \\ \vdots & \vdots & \ddots & \vdots \\ o_{i1} & o_{i2} & \cdots & o_{ij} \end{pmatrix} \otimes \begin{pmatrix} E_{\alpha} \\ E_{\beta} \\ \vdots \\ E_{ij} \end{pmatrix} = \begin{pmatrix} O_{\alpha}E_{\alpha} & O_{\beta}E_{\alpha} & \cdots & O_{ij}E_{\alpha} \\ O_{\alpha}E_{\beta} & O_{\beta}E_{\beta} & \cdots & O_{ij}E_{\beta} \\ \vdots & \vdots & \ddots & \vdots \\ O_{\alpha}E_{ij} & O_{\beta}E_{ij} & \cdots & O_{ij}E_{ij} \end{pmatrix} \tag{1} \\
 & = O_{ij}E_{ij} \\
 & \simeq \text{MCP Label}
 \end{aligned}$$

**Table 1** DNN Model parameters

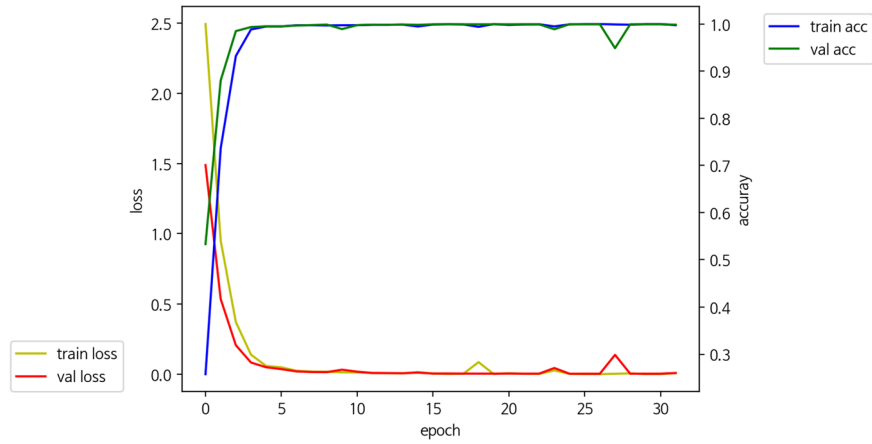
DNN parameter	DNN1	DNN2	DNN3
Hidden layers	[128,64]	[128,64,32]	[32,16,8]
Activation	Relu		
Output dense layers	37		
Output activation	Softmax		
Optimizer	Adam		
Loss	Categorical crossentropy		
Batchsize	16		
Epoch	100		

**Table 2** DNN Model accuracy & loss

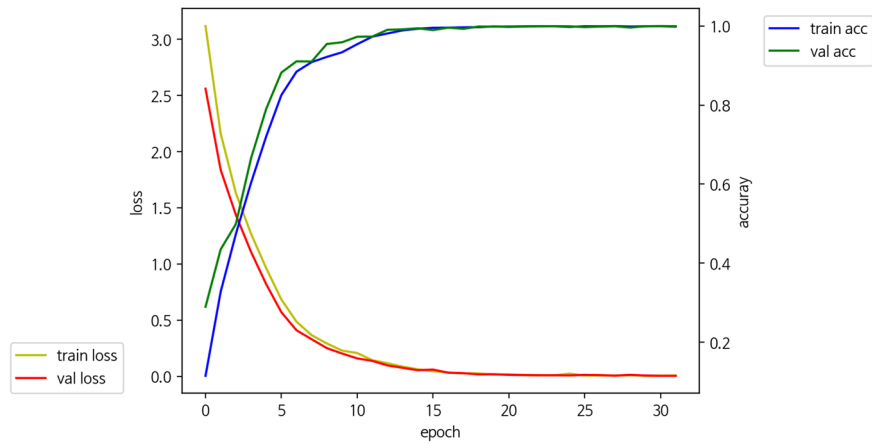
	Train accuracy	Test accuracy	Train loss	Test loss
DNN1	1.00	0.99	0.00006	0.0001
DNN2	0.99	0.99	0.002	0.008
DNN3	0.99	0.99	0.002	0.003



(a) DNN1 model performances



(b) DNN2 model performances



(c) DNN3 model performances

Fig. 7 DNN model performances

S.P.MCPL Algorithm

---

**Algorithm 2:** Spectrogram Pattern MCPL Algorithm

---

```

Data: Raw Signal Vibration Data, Operation State, Environment State
Result: S.P.MC Pattern& S.P.MCP Label
Def Spectrogram Data Cleaning (Raw Sensor Signal Data):
    # Short-time Fourier Transform(STFT)-based Spectrogram for analyzing the frequency
    component of a signal as it changes over time.
    df = Raw Sensor Signal Data
    Fs=4000
    f, tt, Sxx = STFT-spectrogram(df, Fs)
    Spectrogram image = Transform Spectrogram image(tt, f, Sxx, shading)
    S = np.array(spectrogram image)
    Spectrogram pixel value = S.astype("float") / 255.0
    return Spectrogram pixel value
Def MCPLabeling(Operatiomstate, Environmentstate):
    O_state = Operation state
    E_state = Environment state
    # Subset of patterns
    {Spectrogram Pattern} ⊃ {Power pattern 1, Power pattern 2, ..., Power pattern n}
    # labeling multi combination pattern by operation and environment state
    for i in range (len(O_state)) do
        Oi = O[i]
        for j in range (len(E_state)) do
            Ej = E[j]
            MCP Label = Oi ⊗ Ej
    return MCP Label
Def S.P.MCPLDataset (Spectrogrampixelvalue, MCPLLabel):
    # Make S.P.MCPL dataset
    for n in range (len(MCPLLabel)) do
        Spectrogram Pattern = Spectrogram pixel value[n]
        Label = MCP Label[n]
        S.P.MCPL dataset[n] = [SpectrogramPattern, Label]
    return S.P.MCPL dataset
Def Build CNN Model (RawSensorSignalData, OperationState, EnvironmentState):
    SPMCPL Model = CNN network(
        S.P.MCPLDataset(Spectrogram Data Cleaning(Raw Sensor Signal Data),
            MCP Labeling(Operation State, Environment State)))
    return SPMCPL Model(Raw Sensor Signal Data)
Def S.P.MCPL Detection (SPMCPL Model, RawSensorSignalData):
    # Pattern and Label Extraction using SPMCPL Model
    NewDataset = Spectrogram Data Cleaning(Raw Sensor Signal Data)
    SPMCPL Model.predict(NewDataset)
    return S.P.MC Pattern, S.P.MCP Label

```

---

**Table 3** CNN model parameters

CNN model	CNN1	CNN2	CNN3
Filters	[16,128]	[ 32,64 ]	[ 50,100 ]
convolution kernels	3	5	3
Activation	Relu		
Padding	Same		
Drop out	0	0	0.25
Flatten dense layers	32	.	.
Flatten activation	SoftMax		
Optimizer	Adam	Adam	Nadam
Learning rate	0.001	0.002	0.001
Loss	Categorical Crossentropy		
Batchsize	16		
Epoch	100		

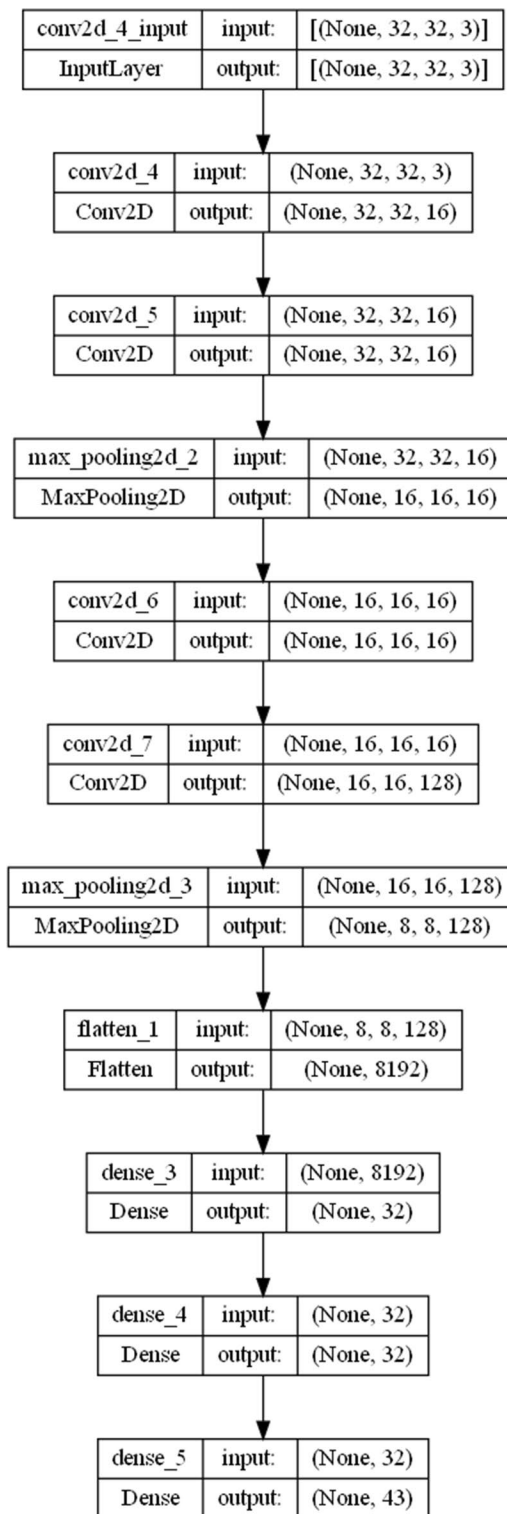
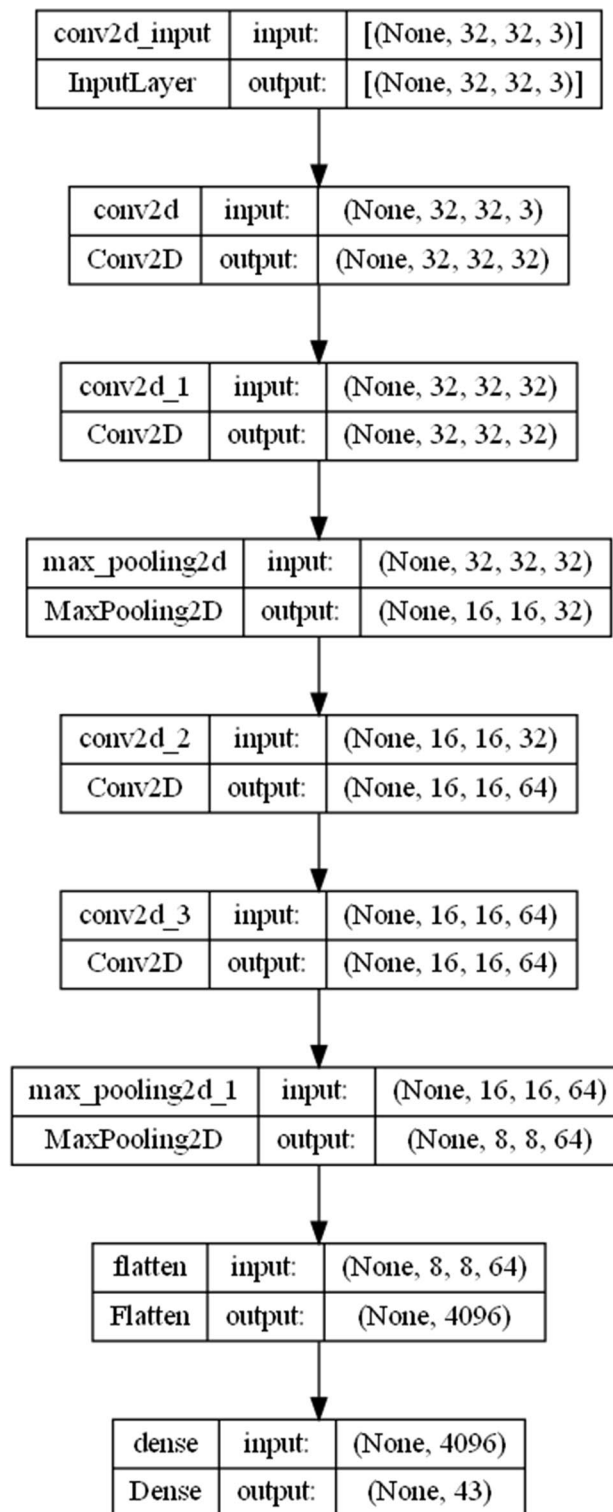


Fig. 8 CNN1 Architecture



**Fig. 9** CNN2 Architecture

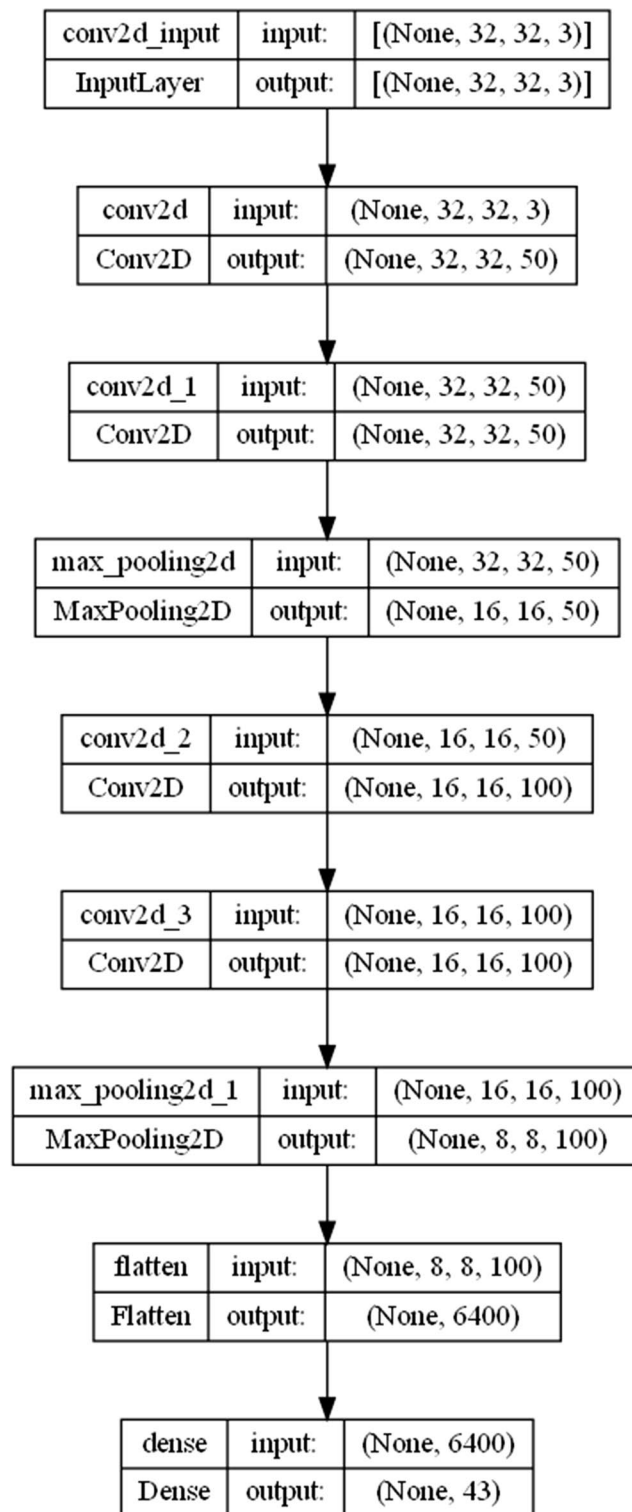


Fig. 10 CNN3 Architecture

This section describes the “S.P.MCPL algorithm”. The FFT transformation of the F.P.MCPL algorithm is effective for analyzing signals in the frequency domain, but it is not effective in determining when the frequency components exist in signal data that changes over time, such as in rotary machines. Thus, it is impossible to determine when a fault has occurred. Therefore, in this algorithm, the first module used is Time-Frequency analysis through the STFT method, which divides the raw sensor signal data into short time intervals and performs a Fourier transformation on the data of each interval. Through this, a Spectrogram image based on STFT can be extracted that visually represents how the frequency components change over time and the color intensity of each pixel of the frequency value in spectrogram extract a value between 0 and 255 for each channel. The second module is MCP Labeling, which derives combined labels that take into account both the operation state and environment state, similar to Eq. (1) mentioned in the “F.P.MCPL algorithm”. The third module create the Spectrogram Power Multi Combination Pattern Labeling(S.P.MCPL) dataset from the Spectrogram pixel values(Input) returned in the first module with the MCPL(Output) in the second module. The fourth module demonstrates the validation of the proposed S.P.MCPL by generating the STFT-Spectrogram-based MCPL dataset through the trained CNN network using either a pre-generated dataset or real-time inputs of raw sensor signal data, operation state, and environment state. Finally, the system can obtain S.P.MC Pattern and S.P.MCP Label to classify the real-time state of the rotary machine by converting incoming signal data into Spectrogram image and loading the built model.

### Verification of MCPL model

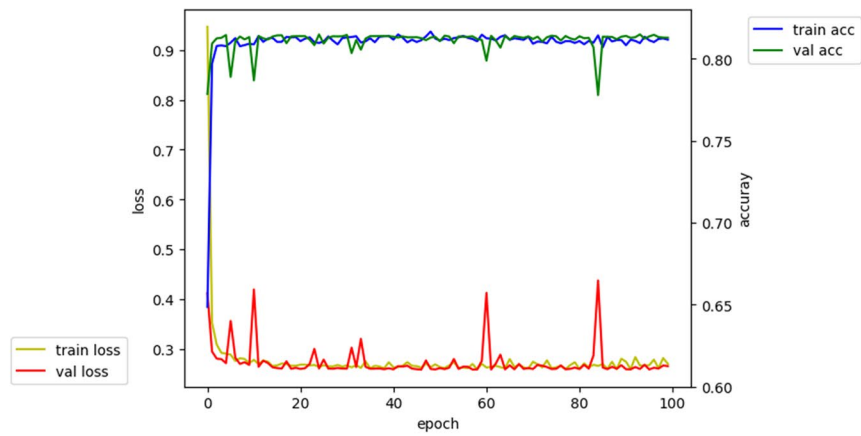
For sensor data, which are traditionally collected in chronological order, a long short-term memory and recursive neural network-based model was conducted that can classify and predict labels by considering the passage of time and the importance of previous and subsequent data values in the time domain. However, frequency domain values and patterns is more important to consider patterns extraction and classification of them, rather than focusing on the importance of data values in the time domain. Therefore, MCPL dataset with frequency patterns and pattern criteria labels is appropriate for applying classification and pattern extraction model for verification of the dataset. Therefore, this paper used DNN for anomaly detection and classification of states to verify F.P. MCPL dataset and CNN for S.P. MCPL dataset.

### DNN Verification for F.P. MCPL dataset

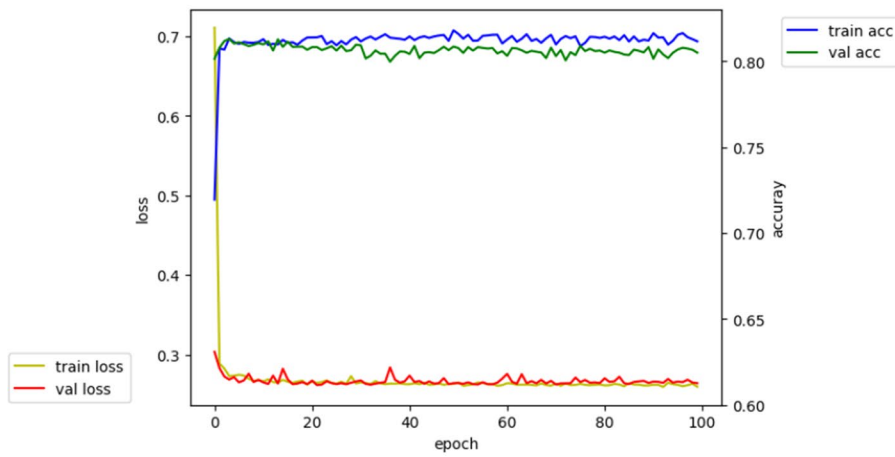
DNN classification model was applied to verify F.P. MCPL datasets. Since F.P. MCPL dataset is constructed of numerical values of frequency for F.P. Pattern, DNN model was used for verification process. Model parameters for DNN structures were set by changing the number of layers and epochs for the stable datasets learning. For DNN

**Table 4** CNN Model accuracy & loss

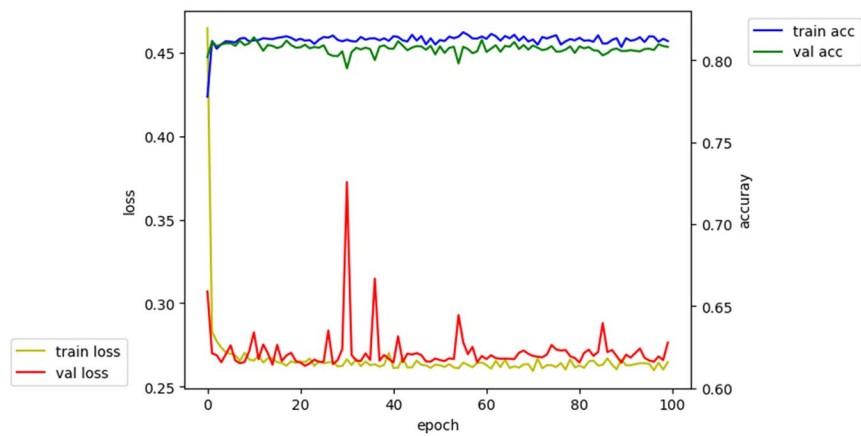
	Train accuracy	Test accuracy	Train loss	Test loss
CNN1	0.814	0.812	0.261	0.265
CNN2	0.817	0.808	0.258	0.266
CNN3	0.812	0.808	0.267	0.276



(a) CNN1 model performances



(b) CNN2 model performances



(c) CNN3 model performances

Fig. 11 CNN model performances

experiment, F.P.MCPL dataset size is 18,500 which constructed 500 data per each MCPL. train set with the size of 0.7 and test with the size of 0.3. Parameters and options are shown in Table 1. DNN1 has 128 and then 64 neurons for hidden layers, DNN2 is added to 32 neurons and DNN 3 has 32,16, and 8 layers. ReLU was applied for the activation function. In the process of the compile, all DNN is set to Adam for optimizer and categorical cross entropy for loss function for multi label classification. In learning step, the batch size is set to 16 (for memory problem) and epoch to 100.

Each accuracy and loss values are described in Table 2 and graphs are in Fig. 7 and it represented that F. P. MCPL labels makes adequate datasets for fluent anomaly detection and classification of rotary machine states under dynamic rotary machine environment.

#### **CNN Verification for S.P. MCPL dataset**

S.P. MCPL dataset is verified with CNN in that the dataset is constructed spectrogram images. For CNN experiment, S.P.MCPL dataset size is 42,992 which constructed 1000 images per each MCPL. Train set with the size of 0.7 and test with the size of 0.3. CNN Models parameters were described in Table 3 and each architecture is shown Figs. 8, 9 and 10. All CNN Models were constructed with two convolutional layers are stacked and there are padding to same option for available to border image learning. The pooling layers are set to (2,2) and activation function to ReLu. CNN1: Kernel size is 3 and each layers have 50 and the second layers have 100 filters. CNN2: Kernel size is 5 and each layers have 32 and the second layers have 64 filters. CNN3: Kernel size is 3 and each layers have 16 and the second layers have 128 filters. All pooling layer is constructed by flatten. CNN3 has 32 filters for dense layers different to CNN1 and CNN2. The output dense has 43 filters for available to classify 43 categories. In the compile step, CNN1: Optimizer is Nadam and learning rate is 0.001. CNN2: Optimizer is Adam and learning rate is 0.002. CNN3: Optimizer is Nadam and learning rate is 0.001. All the loss function of CNN model is categorical cross entropy for multi label classification. In learning step, the batch size is set to 16 (for memory problem) and epoch to 100. The results each model are described in Table 4 and graphs are shown Fig. 11, the accuracy of CNN1,2,3 is 0.81~0.82 and loss values are 0.25~0.26.

#### **CNN Confusion matrix**

As results, there are tendency of misclassification due to lower accuracy than DNN Models. Accordingly, confusion report and matrix are calculated through test data prediction values to how and how to classify the MCP(combination patterns) and MCPL(combination pattern labels). As confusion report described in Table 5, 6, 7, almost 100% classification accuracy results on normal, bearing defect and rotation imbalance, while axis misalignment and belt looseness accuracy are lower than other states. In order to analyze these causes, the confusion matrix of axis misalignment and belt looseness defect is produced. Figure. 12 only considers states of the rotating machine, which is not adapting MCPL and Figure. 13 is the results according to MCPL. Figure. 12 represents that axis misalignment pattern is almost misclassified and confused with belt looseness combination patterns. However, as shown to Figure. 13, combination

**Table 5** CNN1 Confusion report

	Precision	Recall	f1-score	Support
Axis_11	0.00	0.00	0.00	300
Axis_22	0.00	0.00	0.00	300
Axis_2d2	0.50	1.00	0.67	300
Axis_30	0.50	1.00	0.01	300
Axis_37	1.00	1.00	1.00	300
Axis_3d75	0.50	0.99	0.67	300
Axis_3d7	0.45	0.11	0.18	300
Axis_5d5	0.50	0.04	0.07	300
Axis_7d5	0.50	0.00	0.00	300
Bearing_11	1.00	1.00	1.00	300
Bearing_15	1.00	1.00	1.00	300
Bearing_18d5	1.00	1.00	1.00	300
Bearing_2d2	1.00	1.00	1.00	300
Bearing_3d7	1.00	1.00	1.00	300
Bearing_5d5	1.00	1.00	1.00	300
Bearing_7d5	1.00	1.00	1.00	300
Belt_11	0.50	0.96	0.65	300
Belt_15	0.50	1.00	0.67	300
Belt_18d5	0.50	1.00	0.67	300
Belt_22	0.50	1.00	0.67	300
Belt_2d2	0.00	0.00	0.00	300
Belt_55	0.50	1.00	0.67	300
Belt_5d5	0.50	0.01	0.01	300
Belt_7d5	0.49	0.87	0.63	300
Normal_11	1.00	1.00	1.00	300
Normal_15	0.99	1.00	1.00	300
Normal_18d5	1.00	1.00	1.00	300
Normal_22	1.00	1.00	1.00	300
Normal_2d2	1.00	0.99	1.00	300
Normal_30	1.00	1.00	1.00	300
Normal_37	1.00	0.00	1.00	300
Normal_3d75	1.00	1.00	1.00	300
Normal_3d7	1.00	0.99	0.99	300
Normal_55	1.00	1.00	1.00	300
Normal_5d5	1.00	1.00	1.00	300
Normal_7d5	1.00	1.00	1.00	300
Rotating_11	1.00	1.00	1.00	300
Rotating_15	1.00	1.00	1.00	300
Rotating_22	1.00	1.00	1.00	300
Rotating_2d2	1.00	1.00	1.00	300
Rotating_3d7	1.00	1.00	1.00	300
Rotating_55	1.00	0.99	1.00	300
Rotating_5d5	1.00	1.00	1.00	300
Accuracy			0.81	12898
Macro avg	0.77	0.81	0.76	12898
Weighted avg	0.77	0.81	0.76	12898

**Table 6** CNN2 Confusion report

	Precision	Recall	f1-score	Support
Axis_11	1.00	0.00	0.01	300
Axis_22	0.45	0.35	0.39	300
Axis_2d2	0.39	0.11	0.18	300
Axis_30	0.47	0.65	0.54	300
Axis_37	1.00	1.00	1.00	300
Axis_3d75	0.49	0.97	0.65	300
Axis_3d7	0.48	0.90	0.36	300
Axis_5d5	0.48	0.75	0.59	300
Axis_7d5	0.00	0.00	0.00	300
Bearing_11	1.00	1.00	1.00	300
Bearing_15	1.00	1.00	1.00	300
Bearing_18d5	1.00	1.00	1.00	300
Bearing_2d2	1.00	1.00	1.00	300
Bearing_3d7	1.00	1.00	1.00	300
Bearing_5d5	1.00	1.00	1.00	300
Bearing_7d5	1.00	1.00	1.00	300
Belt_11	0.44	0.20	0.27	300
Belt_15	0.50	1.00	0.67	300
Belt_18d5	0.50	1.00	0.67	300
Belt_22	0.47	0.57	0.51	300
Belt_2d2	0.48	0.82	0.61	300
Belt_55	0.42	0.25	0.32	300
Belt_5d5	0.23	0.01	0.02	300
Belt_7d5	0.26	0.03	0.06	300
Normal_11	1.00	1.00	1.00	300
Normal_15	0.99	1.00	0.99	300
Normal_18d5	1.00	1.00	1.00	300
Normal_22	1.00	1.00	1.00	300
Normal_2d2	1.00	1.00	1.00	300
Normal_30	1.00	1.00	1.00	300
Normal_37	1.00	1.00	1.00	300
Normal_3d75	1.00	1.00	1.00	300
Normal_3d7	1.00	1.00	1.00	300
Normal_55	1.00	1.00	1.00	300
Normal_5d5	1.00	1.00	1.00	300
Normal_7d5	1.00	1.00	1.00	300
Rotating_11	1.00	1.00	1.00	300
Rotating_15	1.00	0.99	0.99	300
Rotating_22	1.00	1.00	1.00	300
Rotating_2d2	1.00	1.00	1.00	300
Rotating_3d7	1.00	1.00	1.00	300
Rotating_55	1.00	1.00	1.00	300
Rotating_5d5	1.00	1.00	1.00	300
Accuracy			0.81	12898
Macro avg	0.79	0.81	0.77	12898
Weighted avg	0.79	0.81	0.77	12898

**Table 7** CNN3 Confusion Report

	Precision	Recall	f1-score	Support
Axis_11	0.62	0.02	0.03	300
Axis_22	0.40	0.01	0.03	300
Axis_2d2	0.50	0.36	0.41	300
Axis_30	0.50	0.95	0.65	300
Axis_37	1.00	1.00	1.00	300
Axis_3d75	0.50	0.94	0.66	300
Axis_3d7	0.49	0.13	0.20	300
Axis_5d5	0.47	0.17	0.25	300
Axis_7d5	0.50	1.00	0.67	300
Bearing_11	1.00	1.00	1.00	300
Bearing_15	1.00	1.00	1.00	300
Bearing_18d5	1.00	1.00	1.00	300
Bearing_2d2	1.00	1.00	1.00	300
Bearing_3d7	1.00	1.00	1.00	300
Bearing_5d5	1.00	1.00	1.00	300
Bearing_7d5	1.00	1.00	1.00	300
Belt_11	0.49	0.81	0.61	300
Belt_15	0.00	0.00	0.00	300
Belt_18d5	0.50	0.99	0.67	300
Belt_22	0.50	0.98	0.66	300
Belt_2d2	0.50	0.64	0.56	300
Belt_55	0.47	0.02	0.04	300
Belt_5d5	0.53	0.07	0.12	300
Belt_7d5	0.50	0.87	0.63	300
Normal_11	1.00	1.00	1.00	300
Normal_15	1.00	0.99	1.00	300
Normal_18d5	1.00	1.00	1.00	300
Normal_22	1.00	1.00	1.00	300
Normal_2d2	1.00	1.00	1.00	300
Normal_30	1.96	1.00	0.98	300
Normal_37	1.00	1.00	1.00	300
Normal_3d75	1.00	1.00	1.00	300
Normal_3d7	1.00	1.00	1.00	300
Normal_55	0.91	1.00	0.95	300
Normal_5d5	1.00	1.00	1.00	300
Normal_7d5	1.00	1.00	1.00	300
Rotating_11	1.00	1.00	1.00	300
Rotating_15	1.00	1.00	1.00	300
Rotating_22	1.00	1.00	1.00	300
Rotating_2d2	1.00	1.00	1.00	300
Rotating_3d7	1.00	1.00	1.00	300
Rotating_55	1.00	0.90	0.95	300
Rotating_5d5	1.00	1.00	1.00	300
Accuracy			0.81	12898
Macro avg	0.80	0.81	0.77	12898
Weighted avg	0.80	0.81	0.77	12898

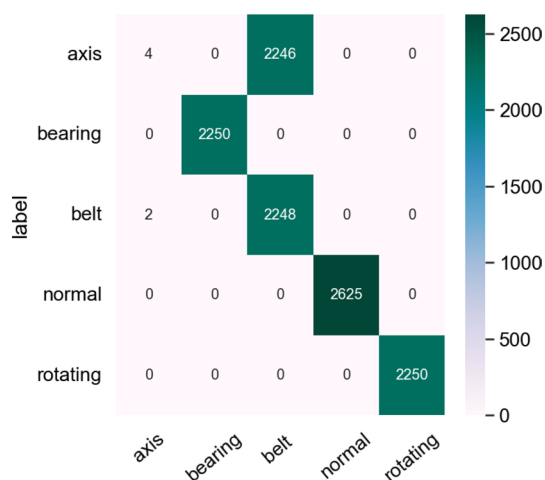
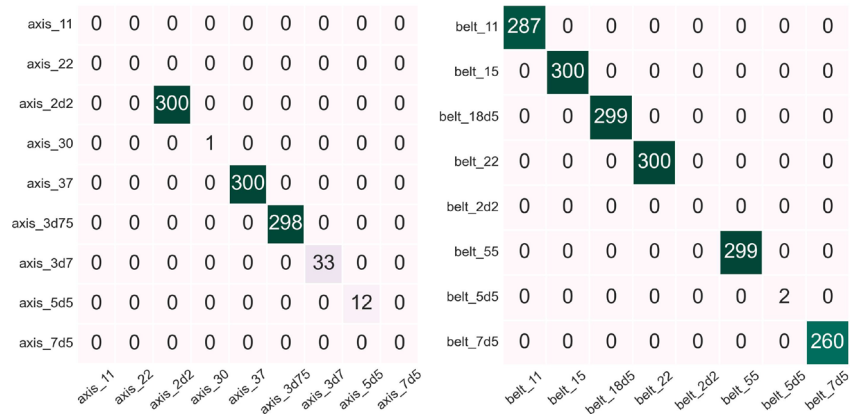


Fig. 12 Only considering States of rotary machine

pattern of axis misalignment state is more classify and easier confusing problem with belt looseness. As a results, MCPL pattern extraction and labeling overcome the miss-classificaion in specific states and it deduces stable results by detailed MCP and MCPL labels.

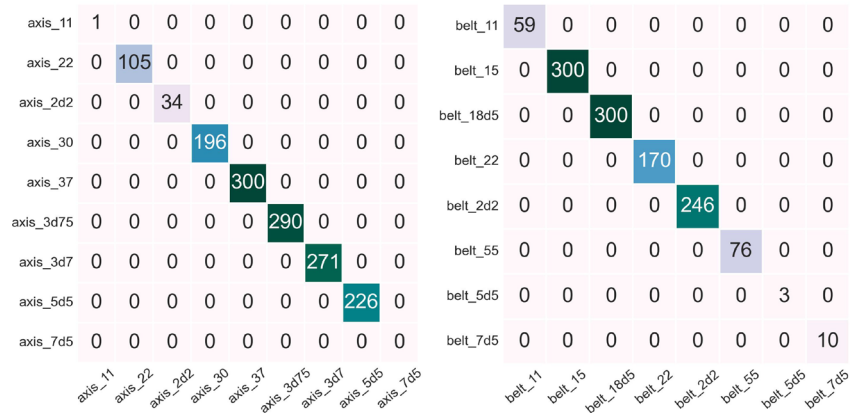
**Conclusion and future work**

This paper suggested MCPL that constructs the learning dataset necessary to deduce accurate diagnosis of rotating machinery conditions. MCPL extracts detailed combination patterns of machinery states and operation power that is possible to overcome the limitation of only considering binary faults (normal or defect), one part of defects and not considering the external environmental factors related to the rotating machinery despite the possibility of identifying distinct vibration patterns by operational capacity under identical conditions. MCPL conducts the process of extracting combination patterns, labels, and learning data sets based on 1. Numerical data and 2. Spectrogram images. 1. MCPL proceeds the FFT to deduce specific vibration patterns based on numerical frequency values. 2. MCPL generates spectrogram images based on STFT time-based frequency values for detecting the vibration patterns based on frequency images. After the process of generating a learning dataset constructed with combination patterns and each label, 1. DNN is adopted for performance evaluation on FFT-based learning dataset and 2. CNN on spectrogram image datasets. DNN shows an accuracy of 0.99 and the loss of 0.0006 and 0.002. CNN presents an accuracy of about 0.82 and a loss of about 0.2 0.3. The confusion matrix. After CNN performance evaluation, the confusion matrix of the recall and F1 score are calculated for identifying the cause of the lower accuracy than DNN. Several types of patterns and label characteristics between axis alignment defect and belt looseness are identified. According to the CNN2 model confusion matrix, there are 258 out of 300 misclassifications of axis alignment-3.7kW defect to belt looseness-7.5kW. On the contrary, 75 of belt looseness - 7.5kW is misclassified to axis alignment-3.7kW. In addition, it is identified that 6 kinds of combination patterns of axis alignment defect and belt looseness are mutually misclassified. Accordingly, It is confirmed that



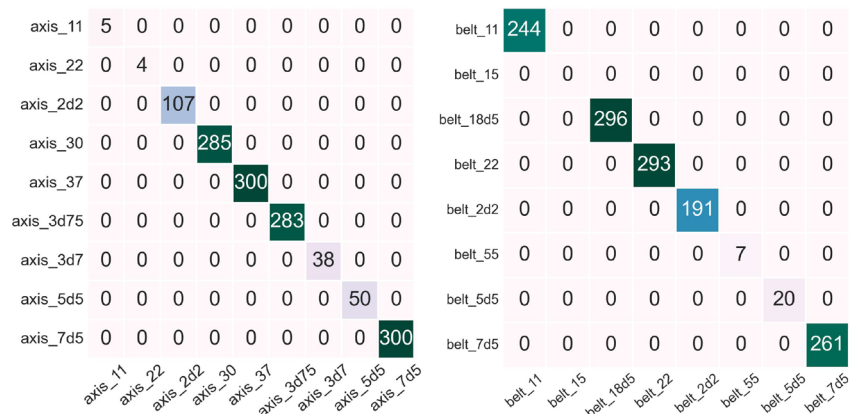
(a.1) CNN1 axis misalignment

(a.2) CNN1 belt looseness



(b.1) CNN2 axis misalignment

(b.2) CNN2 belt looseness



(c.1) CNN3 axis misalignment

(c.2) CNN3 belt looseness

**Fig. 13** Axis & Belt MCPL confusion matrix

the axis alignment defect can be classified almost not classified when only considering the inner states of the rotation machine, and more detailed combination pattern extracting is essential for the identification of misclassification causes. In the next study, we continuously perform detailed combination pattern and labeling studies for more accurate vibration-based diagnosis results. This continuously improved MCPL-based technology would be integrated and expanded to convergence adaptive diagnostic systems with possible to extract various combination patterns in various parts of the machine and operation environment.

#### Acknowledgements

Not applicable.

#### Author contributions

JE and SB conceptualized the research with investigation, designed the methodology and algorithm, created figures for dataset, conducted the experiments, analyzed the results and validation, wrote the main manuscript text including results and figures. YI supervised the completion of the work, contributed to manuscript preparation, funded acquisition and administered project. All authors reviewed the manuscript. All authors read and approved the final manuscript.

#### Funding

This research was supported by the MSIT (Ministry of Science and ICT), Korea, under the ICAN (ICT Challenge and Advanced Network of HRD) program (IITP-2023-RS-2022-00, 156,299) supervised by the IITP (Institute of Information & Communications Technology Planning & Evaluation), by the National Research Foundation of Korea (NRF) grant funded by the Korea government (MSIT). (No. NRF-2023R1A2C1005779).

#### Availability of data and materials

The datasets generated and analyzed during in the current study by utilizing raw data available in the open platform (<https://www.aihub.or.kr/aihubdata/data/view.do?currMenu=115&topMenu=100&aihubDataSe=realM&dataSetSn=238>).

#### Declarations

##### Ethics approval and consent to participate

Informed consent was obtained from all individual participants included in the study.

##### Consent for publication

The authors has consented to the submission of the research report to the journal.

##### Competing interests

The authors declare that they have no competing interests.

Received: 18 October 2022 Accepted: 8 May 2023

Published online: 01 July 2023

#### References

1. International Energy Agency (IEA): IEA Energy Efficiency Series, Paul Waide, Conrad U. Brunner, et al. (Updated Global Energy Consumption Data Based on IEA Statistics for 2014). Paris France (2011). International Energy Agency (IEA)
2. Jeong J-U, Jeong-Ho K. Equipment diagnosis through vibration measurement. *Fire Prot Technol.* 2008;44:30–43.
3. Kafeel A, Aziz S, Awais M, Khan MA, Afaq K, Idris SA, Alshazly H, Mostafa SM. An expert system for rotating machine fault detection using vibration signal analysis. *Sensors.* 2021;21(22):7587.
4. Jiao J, Zhao M, Lin J, Liang K. Hierarchical discriminating sparse coding for weak fault feature extraction of rolling bearings. *Reliab Eng & Syst Saf.* 2019;184:41–54. <https://doi.org/10.1016/j.res.2018.02.010>.
5. Altaf M, Akram T, Khan MA, Iqbal M, Ch MM, Hsu C-H. A new statistical features based approach for bearing fault diagnosis using vibration signals. *Sensors.* 2022;22(5):2012. <https://doi.org/10.3390/s22052012>.
6. Lei X, Wu Y. Research on mechanical vibration monitoring based on wireless sensor network and sparse bayes. *EURASIP J Wireless Commun Netw.* 2020;2020(1):1–13. <https://doi.org/10.1186/s13638-020-01836-9>.
7. Xu K, Li Y, Liu C, Liu X, Hao X, Gao J, Maropoulos PG. Advanced data collection and analysis in data-driven manufacturing process. *Chin J Mech Eng.* 2020;33(1):1–21. <https://doi.org/10.1186/s10033-020-00459-x>.
8. Jan SU, Lee YD, Koo JS. A distributed sensor-fault detection and diagnosis framework using machine learning. *Inf Sci.* 2021;547:777–96. <https://doi.org/10.1016/j.ins.2020.08.068>.
9. Pečar A, Dolenc A, Jaklič A, Peer P, Kovač J. Automatic detection of pronation type of runners using computer vision. *Computer Science.* 2018.
10. Wang J, Chen Y, Hao S, Peng X, Hu L. Deep learning for sensor-based activity recognition: a survey. *Pattern Recognit Lett.* 2019;119:3–11.
11. Park N-C, Koo JS. A study on vibration parameters for the diagnosis of air compressor bearing failure of urban railway vehicles. *Korean Soc Railway.* 2021;9(4):1065–74.

12. Kim S-I, Noh Y, Kang Y-J, Park S, Ahn B. Fault classification model based on time domain feature extraction of vibration data. *J Comput Struct Eng Inst Korea*. 2021;34(1):25–33. <https://doi.org/10.7734/COSEIK.2021.34.1.25>.
13. Jung S-M, Choi W-J. A study on deep learning-based fault diagnosis using vibration data of wind generator. *JKIIT*. 2022;20(6):129–36. <https://doi.org/10.14801/jkiit.2022.20.6.129>.
14. Eraliev O, Lee K-H, Lee C-H. Vibration-based loosening detection of a multi-bolt structure using machine learning algorithms. *Sensors*. 2022;22(3):1210. <https://doi.org/10.3390/s22031210>.
15. Wang L-H, Zhao X-P, Wu J-X, Xie Y-Y, Zhang Y-H. Motor fault diagnosis based on short-time fourier transform and convolutional neural network. *Chin J Mech Eng*. 2017;30(6):1357–68. <https://doi.org/10.1007/s10033-017-0190-5>.
16. Kang K-W, Lee K-M. Cnn-based automatic machine fault diagnosis method using spectrogram images. *J Inst Converg Signal Process*. 2020;21(3):121–6.
17. Viola J, Chen Y, Wang J. Faultface: deep convolutional generative adversarial network (dcgan) based ball-bearing failure detection method. *Inf Sci*. 2021;542:195–211. <https://doi.org/10.1016/j.ins.2020.06.060>.
18. Wang X, Wang T, Ming A, Han Q, Chu F, Zhang W, Li A. Deep spatiotemporal convolutional-neural-network-based remaining useful life estimation of bearings. *Chin J Mech Eng*. 2021;34(1):1–15. <https://doi.org/10.1186/s10033-021-00576-1>.
19. Liu C, Meerten Y, Declercq K, Gryllias K. Vibration-based gear continuous generating grinding fault classification and interpretation with deep convolutional neural network. *J Manuf Process*. 2022;79:688–704. <https://doi.org/10.1016/j.jmapro.2022.04.068>.
20. Li S-Y, Gu K-R. A smart fault-detection approach with feature production and extraction processes. *Inf Sci*. 2020;513:553–64. <https://doi.org/10.1016/j.ins.2019.11.010>.
21. Thuan ND, Hue NT, Vuong PQ, Hong HS. Intelligent bearing fault diagnosis with a lightweight neural network In 2022 11th International Conference on Control, Automation and Information Sciences (ICCAIS). Piscataway: IEEE. 2022;261–266.
22. Hasan MJ, Islam MM, Kim J-M. Bearing fault diagnosis using multidomain fusion-based vibration imaging and multi-task learning. *Sensors*. 2021;22(1):56. <https://doi.org/10.3390/s22010056>.
23. Li Y, Cheng G, Pang Y, Kuai M. Planetary gear fault diagnosis via feature image extraction based on multi central frequencies and vibration signal frequency spectrum. *Sensors*. 2018;18(6):1735. <https://doi.org/10.3390/s18061735>.
24. Li J, Liu Y, Li Q. Intelligent fault diagnosis of rolling bearings under imbalanced data conditions using attention-based deep learning method. *Measurement*. 2022;189: 110500. <https://doi.org/10.1016/j.measurement.2021.110500>.
25. Kumar A, Vashishtha G, Gandhi C, Zhou Y, Glowacz A, Xiang J. Novel convolutional neural network (ncnn) for the diagnosis of bearing defects in rotary machinery. *IEEE Trans Instrum Meas*. 2021;70:1–10.
26. Wu H, Huang A, Sutherland JW. Condition-based monitoring and novel fault detection based on incremental learning applied to rotary systems. *Procedia CIRP*. 2022;105:788–93.
27. Sohaib M, Kim J-M. A robust deep learning based fault diagnosis of rotary machine bearings. *Adv Sci Lett*. 2017;23(12):12797–801.

### Publisher's Note

Springer Nature remains neutral with regard to jurisdictional claims in published maps and institutional affiliations.

Submit your manuscript to a SpringerOpen<sup>®</sup> journal and benefit from:

- Convenient online submission
- Rigorous peer review
- Open access: articles freely available online
- High visibility within the field
- Retaining the copyright to your article

---

Submit your next manuscript at ► [springeropen.com](https://www.springeropen.com)

---